Plant, Cell & Environment

Plant, Cell and Environment (2013) doi: 10.1111/pce.12185

*Mt*ZR1, a PRAF protein, is involved in the development of roots and symbiotic root nodules in *Medicago truncatula*

JULIE HOPKINS[1,2,3]*, OLIVIER PIERRE[1,2,3]*, THÉOPHILE KAZMIERCZAK[4], VÉRONIQUE GRUBER[4,5], FLORIAN FRUGIER[4], MATHILDE CLEMENT[1,2,3], PIERRE FRENDO[1,2,3], DIDIER HEROUART[1,2,3] & ERIC BONCOMPAGNI[1,2,3]

[1]INRA 1355, UMR 'Institut Sophia Agrobiotech', Sophia-Antipolis Cedex, F-06903, France, [2]CNRS 7254, UMR 'Institut Sophia Agrobiotech', Sophia-Antipolis Cedex, F-06903, France, [3]UMR 'Institut Sophia Agrobiotech' Université de Nice-Sophia Antipolis (UNS), Cedex F-06903, France, [4]Centre National de la Recherche Scientifique, Institut des Sciences du Végétal (ISV), Gif-Sur-Yvette Cedex F-91198, France and [5]Les Grands Moulins, 16 rue Marguerite Duras, Université Paris Diderot Paris 7, Paris Cedex 13 F-75205, France

ABSTRACT

PRAF proteins are present in all plants, but their functions remain unclear. We investigated the role of one member of the PRAF family, *Mt*ZR1, on the development of roots and nitrogen-fixing nodules in *Medicago truncatula*. We found that *MtZR1* was expressed in all *M. truncatula* organs. Spatiotemporal analysis showed that *MtZR1* expression in *M. truncatula* roots was mostly limited to the root meristem and the vascular bundles of mature nodules. *MtZR1* expression in root nodules was down-regulated in response to various abiotic stresses known to affect nitrogen fixation efficiency. The down-regulation of *MtZR1* expression by RNA interference in transgenic roots decreased root growth and impaired nodule development and function. *MtZR1* overexpression resulted in longer roots and significant changes to nodule development. Our data thus indicate that *MtZR1* is involved in the development of roots and nodules. To our knowledge, this work provides the first *in vivo* experimental evidence of a biological role for a typical PRAF protein in plants.

Key-words: nitrogen-fixing symbiosis; plant microbe interaction; *Sinorhizobium meliloti*.

INTRODUCTION

Plants often establish symbiotic relationships with specific fungi and bacteria, to enable them to acquire nutrients to support growth and development. Leguminous plants interact with soil bacteria, known as rhizobia, to produce a particular root organ, the nodule, in which the rhizobia reduce atmospheric N_2 to ammonia (NH_3), which is then exported to and assimilated by the plant. In the model legume *Medicago truncatula*, the nodule primordium is initiated from root cortical cells during the initial infection process. The persistent activity of this meristem results in the development of elongated indeterminate nodules. These nodules consist of four main zones (from the tip to the base of the nodule): zone I, the apical meristematic zone responsible for the continuous growth of the nodule over many weeks; zone II, the infection zone, in which bacteria from infection threads are released into plant cells; zone III, the fixation zone, in which bacteria that have differentiated into nitrogen-fixing bacteroids reduce atmospheric N_2 to NH_3; and zone IV, the senescence zone, in which both symbionts degenerate (Timmers *et al.* 2000). Exchanges between the root nodule and other plant organs are mediated by well-developed vascular tissues at the periphery of the nodule. Intensive research has focused on the molecular dialogue between the two partners in the establishment of this symbiotic association, including dissection of the Nod factor signalling pathway (Jones *et al.* 2007; Gibson, Kobayashi & Walker 2008; Oldroyd *et al.* 2011).

Many environmental stresses affect nodule functioning, potentially leading to nitrogen fixation defects and slowing the development of the plant. We previously identified a gene, *GmG93*, that is specifically expressed in functioning nodules and transiently repressed under drought stress in soybean (Clement *et al.* 2006). The deduced amino acid sequence of the protein encoded by *GmG93* is similar to those of proteins of the *Arabidopsis* PRAF family (Jensen *et al.* 2001; Heras & Drobak 2002; van Leeuwen *et al.* 2004). The PRAF (PH, RCC1 and FYVE) protein family is a family of proteins specific to plants, with a distinctive domain architecture and various unique sequence traits (Wywial & Singh 2010), but with no known physiological function. PRAF proteins typically have four characteristic domains: two lipid-binding domains: the PH domain (pleckstrin homology) and the FYVE (Fab 1, YOTB, Vac 1 and EEA1) zinc-finger domain, in the N-terminal and central regions, respectively, seven repeats of the RCC1 (regulator of chromatin condensation) motif, which is also known as the ATS1 (alpha-tubulin suppressor) domain and finally, a C-terminal BRX/DZC (*brevis radix*/disease resistance, zinc finger, chromosome condensation) domain (Jensen *et al.* 2001; Heras & Drobak 2002; Briggs, Mouchel & Hardtke 2006; Wywial & Singh 2010). In *Arabidopsis thaliana*, the PRAF family has nine members, all with a similar protein structure (van Leeuwen *et al.* 2004). However, no particular change in phenotype has ever been observed for any *Arabidopsis* PRAF mutant line (http://www.arabidopsis.org/).

Correspondence: E. Boncompagni. Fax: +33 (0) 492 386 587; e-mail: boncompa@unice.fr

*Julie Hopkins and Olivier Pierre contributed equally to this work.

We assessed the importance of the *GmG93* homolog *MtZR1* for root growth and the symbiotic process in *M. truncatula*. Using genetic approaches, we showed that *Mt*ZR1 was involved in root and nodule development.

MATERIALS AND METHODS

Plant materials, growth procedures and nodulation assays

M. truncatula cv. Jemalong A17 seeds were surface-sterilized and germinated, as previously described (Boisson-Dernier *et al*. 2001). Wild-type *Medicago* and composite plants with transgenic roots were grown in a phytotron, watered with nitrogen-free nutrient medium (Puppo, Dimitrijevic & Rigaud 1982) and inoculated 5 d after germination with *Sinorhizobium meliloti* strain 102F34 (Osteras *et al*. 1998). Plants were maintained under a 16 h light/8 h dark regime, at temperatures of 23 °C during the light phase and 21 °C during the dark phase. The following chemical treatments were applied to 6-week-old nodulated plants for 5 d: NaCl (250 mM), CdCl (100 μM), NO_3NH_4 (10 mM). Alternatively, plants were subjected to drought stress for 3 d. Abiotic stress conditions were defined on the basis of previous studies (Matamoros *et al*. 1999; Clement *et al*. 2006; Staudinger *et al*. 2012). Nodulated plants were harvested for physiological experiments. Nodules were fixed for histochemical experiments or frozen in liquid N_2 and stored at −80 °C for further molecular analysis. For hormonal treatments, 15 germinated seedlings (*M. truncatula* cv. Jemalong A17) were placed on a grid in a Magenta box with 30 mL of low-nitrogen 'i' medium. They were grown for 5 d in an incubator, with shaking (125 r.p.m.), at 24 °C, under long-day conditions (16 h light/8 h dark), as described by Gonzalez-Rizzo, Crespi & Frugier (2006). They were then treated with 10^{-7} M indole-3-acetic acid (IAA), 10^{-7} M 1-aminocyclopropane-1-carboxylic acid (ACC), 10^{-7} M benzylaminopurine (BAP) or 10^{-7} M abscisic acid [ABA; all obtained from Sigma-Aldrich (St Louis, MO, USA)], and incubated under the same growth conditions for various times (0, 1 and 3 h). Bioactive hormonal conditions were defined on the basis of previous studies (Gonzalez-Rizzo *et al*. 2006; Ariel *et al*. 2010; Plet *et al*. 2011).

Bacterial strains

All the strains used in this study were grown on Luria-Bertani medium supplemented with appropriate selective antibiotics, at 28 °C (*Sinorhizobium* and *Agrobacterium* strains) or 37 °C (*Escherichia coli*; Supporting Information Table S2). *Agrobacterium rhizogenes* strain A4S was used to transform *M. truncatula*. The binary vectors were introduced into A4S by electrotransformation, and colonies carrying these vectors were selected by growth on spectinomycin (100 μg mL^{-1}) for 2 d.

N_2 fixation

An acetylene reduction assay (ARA) was carried out 6 weeks after inoculation, on biological triplicates, with at least 12 nodulated roots per replicate (about 20 nodules per root), by assessing acetylene reduction to ethylene *in vivo*, as previously described (El Msehli *et al*. 2011).

ZR1 promoter::*GUS* construct

The *MtZR1* gene is located on the fully sequenced BAC mth2-32h21 (GenBank accession AC151822), and on *M. truncatula* chromosome 3. The complete *MtZR1* mRNA sequence was determined by aligning the Chr3 sequence with the *MsZR1*cDNA, using the NCBI Spidey program (http://www.ncbi.nlm.nih.gov/IEB/Research/Ostell/Spidey/spideyweb.cgi). The *MtZR1* promoter was obtained by PCR amplification from genomic DNA with the primers PMtZR1-F and PMtZR1-R (Supporting Information Table S3). These primers amplify a 2130 bp DNA fragment located upstream from the translational start codon of *MtZR1*. This PCR-amplified DNA fragment was cloned, verified by sequencing and inserted into the pDON207 donor vector and then into pKGWFS7 (VIB, Ghent, Belgium), with Gateway Technology (Life Technologies SAS, Saint Aubin, France).

ZR1 overexpression and RNAi constructs

The full-length *MsZR1* coding sequence from pBluescript SK$^{(-)}$-*MsZR1* (AJ409163, kindly provided by K. Zwerger, Vienna, Austria), digested with *Sac*I and *Xho*I, was inserted into the pENTR4 donor vector. The corresponding 3.7 kb insert was then inserted into an overexpression vector, pK7WG2D (VIB), with Gateway Technology (Invitrogen; *P35S::ZR1*, Supporting Information Table S2). A control plasmid was constructed in a similar manner, by insertion of the GUS cassette from a pENTR-GUS donor vector (Invitrogen; *P35S::GUS*, Supporting Information Table S2). The RNAi construct was obtained by amplifying the *MtZR1* 5′UTR with the 5′UTRZR1-F and 5′UTRZR1-R primers, to generate a 256 bp PCR product (Supporting Information Table S3). This PCR product was inserted into a pGEM-T® vector (Promega, Charbonnières-les-bains, France), from which it was released by digestion with *Nco*I and *Not*I and inserted into a pENTR4 donor vector (Invitrogen). Finally, the *ZR1* 5′UTR insert was inserted into pK7GWIWG2D(II),0 (VIB), with Gateway Technology (*P35S::RNAiZR1*, Supporting Information Table S2). As a control, the empty vector pK7GWIWG2D(II),0 was used for RNAi experiments.

ZR1 fusion protein constructs

The full-length *MsZR1* ORF from pENTR4-*MsZR1* was inserted into pK7FWG2 (VIB) with Gateway Technology (Invitrogen; *P35S::ZR1::GFP*, Supporting Information Table S2).

RNA extraction and RT-qPCR analysis

Total RNA was isolated from plant material by the single-step method, with acid guanidinium thiocyanate (Chomczynski &

Sacchi, 1987). Total RNA (1 μg) was then subjected to DNase I treatment (Fisher Scientific, Illkirch Cedex, France). The absence of genomic DNA contaminations in the RNA samples was tested by PCR analysis of all samples using oligonucleotides bordering an intron in the *Leghemoglobin I* gene of *M. truncatula*. Reverse transcription was performed on 2 μg of total RNA, with the Omniscript II reverse transcriptase (Invitrogen). Quantitative PCR with SyberGreen (Eurogentec, Angers, France) was followed on an Opticon Monitor 3 (Bio-Rad, Hercules, CA, USA), in a 15 μL reaction mixture containing 300 nM of each primer (Supporting Information Table S2). We performed qPCR on a DNA Engine OPTICON 2 cycler (MJ Research, Waltham, MA, USA), with the following parameters: 2 min at 50 °C, 10 min at 95 °C and then 39 cycles of 15 s at 95 °C, 1 min at 60 °C. Reactions were performed in triplicate and the results averaged. The primers used (Supporting Information Table S3) had a calculated melting temperature of 59 to 62 °C and were unique in the MTGI (TIGR) and Medicago EST Navigation System (Journet *et al.* 2002) databases. Relative expression level was calculated as a normalized gene expression ratio with respect to the constitutively expressed *Mtc27* (El Msehli *et al.* 2011) and *MtRP40S* [40S ribosomal protein S8 genes (Fedorova *et al.* 2002)] or *MtACT* (actin 11) and *MtRBP1* (RNA-binding protein 1; Plet *et al.* 2011) genes, according to the $2^{2\Delta\Delta}$CT method (Livak & Schmittgen 2001). The stability of the reference genes in transgenic conditions was checked with the GeNorm software (Vandesompele *et al.* 2002). The significance of differences in expression was assessed with the REST 2009 software (Pfaffl, Horgan & Dempfle 2002). Comparison with experimental control conditions was carried out to determine fold changes in expression.

Transient expression of a recombinant fusion protein construct in tobacco leaves

Nicotiana tabacum plants were grown under continuous light for 1 month at 26 °C. Tobacco leaves were infiltrated with *A. tumefaciens* AGL1 (Lazo, Stein & Ludwig 1991), as previously described (Voinnet *et al.* 2003), and plants were analysed 2 d after agroinfiltration. GFP fluorescence was monitored by confocal microscopy (Zeiss LSM510 microscope, Carl zeiss, Le Pecq, France). In cases of treatment with a protease inhibitor to decrease protein degradation, the agroinfiltrated leaves were treated with 2 mM E64d (Sigma) for 3 h before observation (Takase *et al.* 2003; Hatsugai *et al.* 2004; Caillaud *et al.* 2009).

Root transformation and hairy root growth measurement

Roots were transformed with *A. rhizogenes* A4S (Alpizar *et al.* 2006), by a modified version of method previously described (Vieweg *et al.* 2004). In brief, seeds were allowed to germinate for 24 h at 20 °C and were then transferred to 4 °C for 7 d. Agrotransformation was achieved by injecting a mixture of 1% peptone-sucrose and *A. rhizogenes* into plant hypocotyls. Transgenic roots were allowed to develop for 7 d at 20 °C and were then incubated for 21 d at 25 °C in a phytotron with a 16 h light/8 h dark photoperiod, under a light flux of 360 μmol m^{-2} s^{-1}. The tap root was then removed, leaving only the lateral transgenic roots to develop. A nitrogen-free mineral solution (Puppo *et al.* 1982) was supplied and the roots were then inoculated with 0.05 OD_{600} units of *S. meliloti* 102F34 (Osteras *et al.* 1998). Transgenic roots were screened by GFP epifluorescence when possible. Nodules were harvested four to 7 weeks after inoculation and fixed for histochemical analysis experiments or ground in liquid nitrogen and stored at −80 °C for further molecular analyses. Alternatively, hairy roots were obtained as described by Boisson-Dernier *et al.* (2001). *A. rhizogenes*-transformed *Medicago* roots were excised (1 cm from the tip) and transferred onto SHb10 agar (Ramos & Bisseling 2003). The GFP fluorescence of each transgenic root was checked before selection. Transgenic roots were grown for 3 weeks, at 25 °C, in the dark, and root growth was then evaluated by photographing all plates with a digital camera to produce image files suitable for quantitative analysis with NIH Image J software (v1.42; http://rsb.info.nih.gov/). Analysis of variance (ANOVA) was carried out for statistical assessments of root and nodule growth.

Histological analysis of transgenic tissues

For light microscopy, nodules were fixed in 1% gluteraldehyde, 4% formaldehyde in 0.1 M phosphate buffer at pH 7.2, washed, dehydrated and embedded in Technovit 7100 (Kulzer Histo-Technik, Wehrheim, Germany), according to the manufacturer's instructions. Sections were cut on a microtome (Jung) to yield 5 μm slices, which were mounted in DPX mounting solution (VWR International Ltd, Lille, France). GUS activity was localized, in nodule sections, after overnight incubation with the histochemical substrate 5-bromo-4-chloro-3-indolyl-β-D-glucuronide, cyclohexylammonium salt (Sigma), as described by Journet *et al.* (1994). Dark-field images were taken with an Axioplan2 microscope (Carl Zeiss, Oberkochen, Germany). A general overview of nodule structure was obtained by staining with toluidine blue (Van de Velde *et al.* 2006). For epifluorescence microscopy, 80 μm root sections were cut with a vibratome (HM 650V, Microm International GmbH, Walldorf, Germany), mounted on slides in water and observed directly with an upright microscope. Observations were made and images were recorded with a Zeiss Axioplan2 microscope (Carl Zeiss). Analyses were carried out with Axiovision4 software or the Zeiss confocal system (Zeiss LSM 510 META microscope).

Bioinformatic analyses

The phylogenic analysis was performed on the phylogeny.fr platform (Dereeper *et al.* 2008) in advanced mode, with all the default parameters. The phylogenic tree was reconstructed by the maximum likelihood method, with the protein WAG substitution matrix. The reliability of internal branches was assessed by bootstrapping, with 500 bootstrap replicates. Protein sequence analysis was carried out with Supermatcher (http://emboss.sourceforge.net/).

RESULTS

MtZR1 is a member of the small plant-specific PRAF protein family

We previously identified the *GmG93* gene, which encodes a nodule-specific PRAF protein in *Glycine max*, as a late nodulin gene expressed in nodule-infected cells (Clement *et al*. 2006). A BLAST analysis of protein databases identified proteins with high levels of sequence identity to *Gm*G93 (*Gm*G93: Glyma11g33200.1), not only in other leguminous plants, such as *M. sativa* (*Ms*ZR1: AJ409163), but also in non-leguminous plants, such as *A. thaliana* (*At*PRAF1: AT1G76950; Fig. 1a). Blast analysis of the *M. truncatula* genomic sequence with the *MsZR1* nucleic acid sequence identified five genes on chromosomes 1, 3 and 5 (Fig. 1B, Supporting Information Table S1). The putative proteins encoded by these five genes had similar molecular weights, between 114 and 119 kDa. The PH, RCC1/ATS1, FYVE and BRX/DZC domains were present in all the deduced protein sequences and the encoded proteins were 47% to 69% similar (Fig. 1a). The phylogenic tree of PRAF protein sequences from *A. thaliana*, *O. sativa*, *G. max*, *M. sativa* and *M. truncatula* contained four clusters (Fig. 1b). In *M. truncatula*, *Mt*ZR1 (AC151822_29.5, Supporting Information Table S1) was the protein most similar (98.4%) to *Ms*ZR1 (Supporting Information Fig. S1). We carried out molecular, biochemical and cellular analyses of *Mt*ZR1, with the aim of determining the role of a member of the PRAF protein family in roots and understanding its relevance to the symbiotic process.

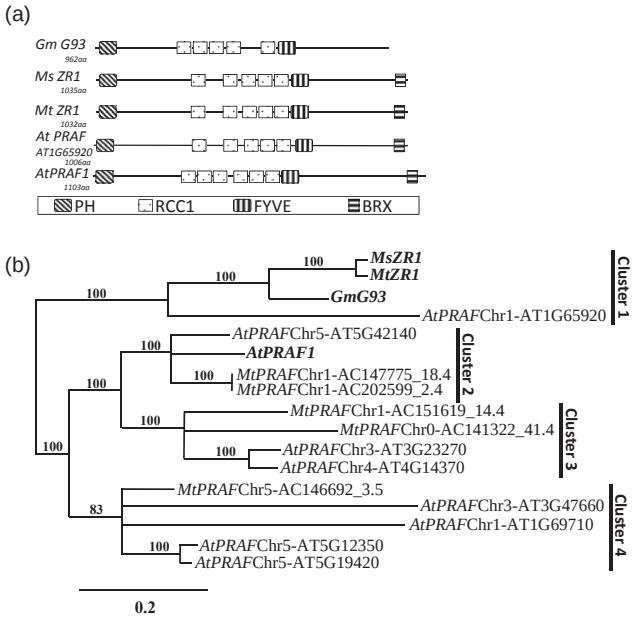

Figure 1. Outline of the structure of selected PRAF/ZR1 proteins and phylogenic tree. (a) The domains of the *Gm*G93 (Glyma11g33200.1), *Ms*ZR1 (AJ409163), *Mt*ZR1 (AC151822_29.5), AtPRAF-AT1G65920 and *At*PRAF1 (AT1G76950) proteins: PH, pleckstrin homology; RCC1, regulator of chromosome condensation; FYVE, zinc-finger protein domains named according to the parental proteins Fab1, YGL023, VSP27 and EEA1; BRX, brevis radix. (b) Phylogenic tree of nine PRAF proteins from *A. thaliana*, five PRAF proteins from *M. truncatula* and PRAF proteins from *G. max*, *O. sativa* and *M. sativa* available from the GenBank database. This analysis was carried out on the phylogeny.fr platform (Dereeper *et al*. 2008) in advanced mode, with all the default parameters). The phylogenic tree was reconstructed by the maximum likelihood method, with the protein WAG substitution matrix. The reliability of internal branches was assessed by bootstrapping, with 500 bootstrap replicates, and values are shown in percentages, with a branching cut-off at 80%.

The *ZR1* gene is expressed in various organs in *M. truncatula* and is regulated at the transcriptional level by various abiotic stresses

We analysed *MtZR1* expression in leaves, roots and 6-week-old nodules, by RT-qPCR. Levels of *MtZR1* expression were similar in leaves, roots and root nodules (Fig. 2a). Unlike *GmG93*, *MtZR1* was not specifically expressed in root nodules. Nevertheless, the expression of *MtZR1* in nodules was significantly down-regulated in response to various abiotic stresses affecting biological nitrogen fixation (BNF) efficiency. *MtZR1* expression levels were more than halved following the exposure of plants to salt, cadmium, ammonium nitrate and drought stresses (Fig. 2b). These results indicate that *MtZR1* is expressed in nitrogen-fixing nodules but is not a nodule-specific gene. Despite its clear down-regulation in response to various abiotic stresses, the expression profile of *MtZR1* in *M. truncatula* differs from that of *GmG93* in soybean.

ZR1 is expressed in roots, the nodule meristem and the vascular bundles of mature nodules

We analysed the pattern of *MtZR1* expression during nitrogen-fixing symbiosis, by isolating a 2130-bp *MtZR1* promoter fragment from *M. truncatula* genomic DNA by PCR amplification and constructing a chimeric *PZR1::GUS* promoter–reporter gene fusion (Supporting Information Tables S2 and S3) and carrying out histochemical analyses of GUS activity in roots and nodules transgenic for this fusion. GUS staining was detected mostly towards the root tip and in the meristem of emerging lateral roots (Fig. 3a–b). In 2-week-old transgenic nodules, GUS staining indicated that *MtZR1* was expressed in the infected zone containing symbiosomes (Fig. 3c–d). In 6-week-old transgenic nodules, strong GUS staining was detected in vascular bundles (Fig. 3e–f, Supporting Information Fig. S3). However, weaker GUS staining was also detected in the meristem, the infection zone and the nitrogen-fixing zone of the 6-week-old nodule (Fig. 3e–f). These results indicate that *MtZR1* is expressed principally in the meristematic zones of roots. In nodules, *MtZR1* is expressed not only in the meristem, but also in the infection and nitrogen-fixing zones and in the vascular bundles of 6-week-old nodules.

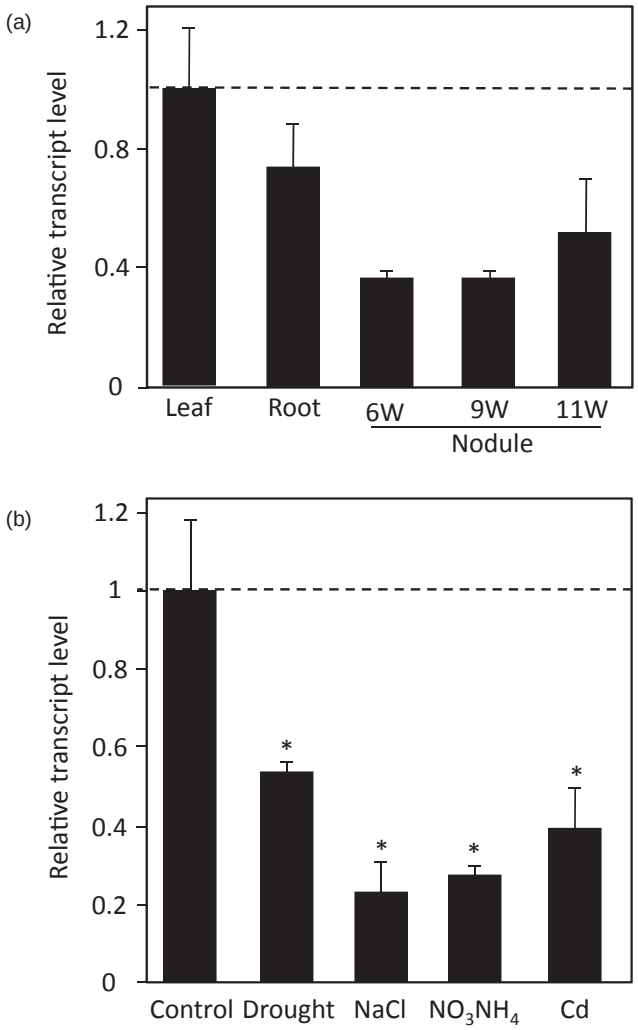

Figure 2. Regulation of *MtZR1* expression in various organs and symbiotic nodules in conditions of abiotic stress. (a) Relative real-time quantitative PCR analysis of *MtZR1* expression (black boxes) in various plant organs (nodules, leaves and roots) at 6 weeks post-inoculation (PI). Fold changes relative to expression in flowers are indicated by a dashed line. (b) Relative RT-qPCR analysis of *MtZR1* expression at 6 weeks PI, in plants subjected to various abiotic stresses for 1 week. The constitutively expressed reference gene is *Mtc27* (Favery *et al*. 2002). Fold changes relative to non-treated conditions are indicated by a dashed line. For both experiments, means of three biological experiments are shown and error bars indicate the standard error of the mean.

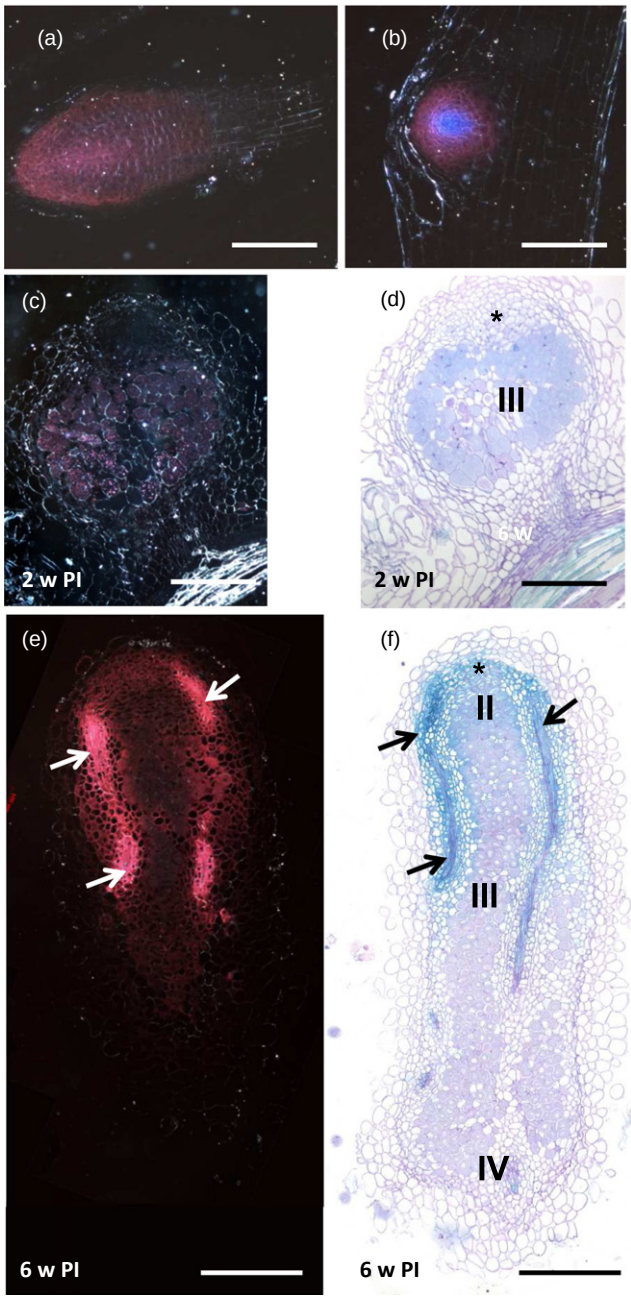

Figure 3. Spatiotemporal regulation of *MtZR1* expression in roots and symbiotic nodules. (a–c) *PMtZR1*::*GFP*::*GUS*; dark-field observation of GUS staining on 5 μm-thick sections of root tissues. Root-tip region (a), lateral root (b) expression. (c–f) Dark-field observation (c and e) or bright (field observation (d and f) of toluidine-*o*-blue staining in transgenic *PMtZR1*::*GFP*::*GUS* root nodules. Sections (5 μm thick) of *PMtZR1*::*GFP*::*GUS* transgenic root nodules from 2- to 6-week-old PI nodules, showing *GUS* expression in infected cells of the root nodule (2 weeks PI, zone III, c–d) and in the nodule vascular bundles (6 weeks PI, white/dark arrows, e–f). Zones I to IV: functional zones in an indeterminate nitrogen-fixing nodule. Scale bars: 800 μm (a to b), 400 μm (c to f).

The *ZR1* protein is located in the cytosol and nucleus

We investigated the distribution of the ZR1 protein *in vivo*, by fusing the ORF of *ZR1* (3.7 kb) to the enhanced green fluorescent protein gene downstream from the CaMV 35S promoter (*P35S*) (Supporting Information Table S2; *P35S::ZR1::GFP*). Accumulation of the resulting protein was poor in transgenic *M. truncatula* roots, so transient expression of the genetic construct was instead achieved by the agroinfiltration of *N. tabacum* leaves. Accumulation of the ZR1::GFP protein was observed by confocal microscopy

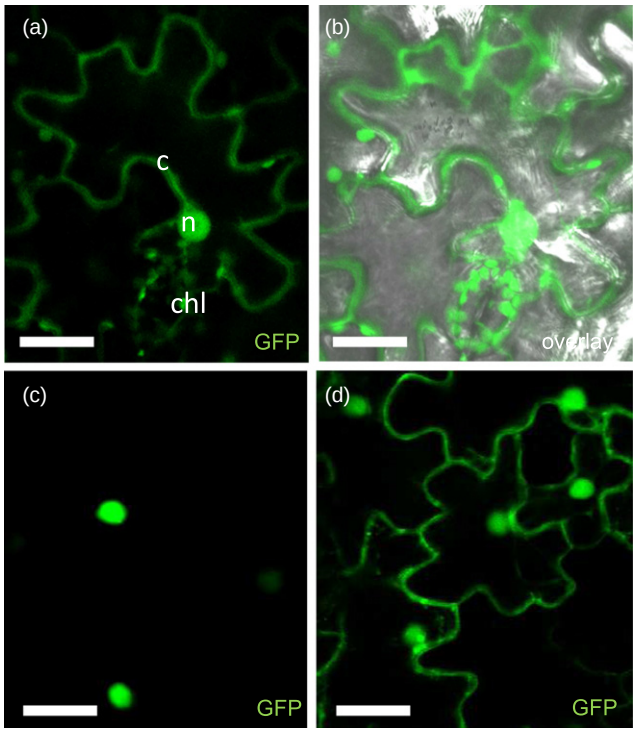

Figure 4. Subcellular localization of the recombinant ZR1::GFP protein in tobacco leaves. (a–b) Confocal images of tobacco epidermal leaf cells infiltrated with *A. tumefaciens* expressing the *P35S*::*ZR1*::*GFP* construct. (a) GFP fluorescence associated with the *P35S*::*ZR1*::*GFP* construct 3 h after treatment with 2 mM E64d. (b) Overlay of the transmission image and GFP fluorescence of tobacco epidermal cells. (c) Nuclear GFP fluorescence associated with the expression of BUBR1::GFP. (d) Cytosolic and nuclear GFP fluorescence associated with BUB3.1::GFP. c, cytoplasm; chl, chloroplast; n, nucleus. Scale bars: 20 μm.

after treatment with a cysteine protease inhibitor, E64-d, for 3 h. In localization experiments, we used BUBR1::GFP as a positive control for an exclusively nuclear distribution and BUB3.1::GFP as a positive control for a nuclear and cytosolic distribution (Caillaud *et al*. 2009); Fig. 4). The ZR1::GFP fusion protein was detected in the cytosol and in the nucleus (Fig. 4a). A similar distribution was observed for BUB3.1::GFP (Fig. 4d), whereas BUBR1::GFP was detected only in the nucleus, as expected. This distribution suggests that ZR1 may be transported to the nucleus.

ZR1 deregulation modifies root and nodule development and nodule functioning

In roots, *ZR1* is expressed mostly in the meristematic zones. We investigated the importance of *ZR1* expression for root development, by analysing the growth rate of transgenic root lines with various levels of *ZR1* expression. We analysed the growth rates of *ZR1*-overexpressing root lines and root lines in which *ZR1* was silenced by RNAi. The efficacy with which genetic constructs modified *ZR1* mRNA levels was checked by RT-qPCR analysis. As expected, *ZR1* expression levels were significantly higher in roots and nodules expressing the *P35S::ZR1* construct than in control tissues carrying the *P35S::GUS* construct, and significantly lower in roots or nodules expressing the RNAi*ZR1* construct than in control tissues carrying the control RNAi empty vector (Supporting Information Fig. S4). The expression of other *MtPRAF* genes was not significantly modified in the transgenic lines (Supporting Information Fig. S5). As the production of composite plants resulted in a large range of *ZR1* expression levels, root growth analysis was performed on multiple root tips from four independent transgenic root lines selected on the basis of *ZR1* expression level and grown on SHb10 medium containing 1.3% agar for 2 weeks. The overexpression of *ZR1* (*P35S::ZR1*) was associated with significantly higher levels of root growth, resulting in longer roots (23% longer) than for the *P35S::GUS* control (Fig. 5a). Moreover, the number of lateral roots (57%) was significantly greater in root lines overexpressing *ZR1* than in *P35S::GUS* control lines (Fig. 5b). By contrast, RNAi*ZR1*-silenced transgenic roots were significantly shorter (31 %) than control roots (Fig. 5a), with no difference in the number of lateral roots (Fig. 5b). As phytohormones play an important role in determining root architecture, we investigated their effects on *ZR1* expression in *Medicago* roots (Fig. 5c). *ZR1* expression seemed slightly repressed by cytokinins (BAP), and induced by auxin (AIA) and abscisic acid (ABA). However, the expression of *ZR1* did not seem significantly regulated by ethylene treatment (ACC). As we found that *ZR1* was also expressed in root nodules, we investigated the importance of *ZR1* expression for nodule development and functioning. We analysed various physiological parameters of 6-week-old nodules from transgenic composite plants of *M. truncatula* (Vieweg *et al*. 2004). No significant difference in nodule number was found between controls and deregulated plants for ZR1 (Supporting Information Fig. S6). *ZR1*-overexpressing nodules were significantly longer than control nodules (Fig. 6a–b) and their weight was correlated with their size. By contrast, nodules in which *ZR1* was silenced by RNAi were significantly smaller than those from control plants (Fig. 6c–d) and this was reflected in lower fresh weight (Fig. 6e–f). Biological nitrogen fixation (BNF) by bacteroids is a good physiological marker of nodule fitness. We performed an acetylene reduction assay (ARA) to analyse the BNF activity of the transgenic nodules (Fig. 7a). Transgenic nodules overexpressing *ZR1* had a significantly higher BNF activity than control transgenic nodules (Fig. 7a). In this assay, we evaluated the amount of ethylene formed per hour and per nodule. By contrast, nodules in which *ZR1* was silenced by RNAi had a lower BNF activity than control transgenic nodules. We investigated the correlation between the BNF activity of transgenic nodules and the expression of genes induced during the functioning and senescence of nodules, by analysing the expression of the leghemoglobin *Lb1* (Ott *et al*. 2005), *NCR001* (Mergaert *et al*. 2003), *ENOD 8* (Coque *et al*. 2008), *CP6* and *VPE* (Van de Velde *et al*. 2006) genes by RT-qPCR. The leghemoglobin *Lb1*, *NCR001* and *ENOD8* genes are expressed in the nitrogen-fixing zone (III), whereas *CP6* and *VPE* encode proteases induced during nodule senescence (IV). The levels of leghemoglobin, *NCR001*, *ENOD 8*, *CP6*

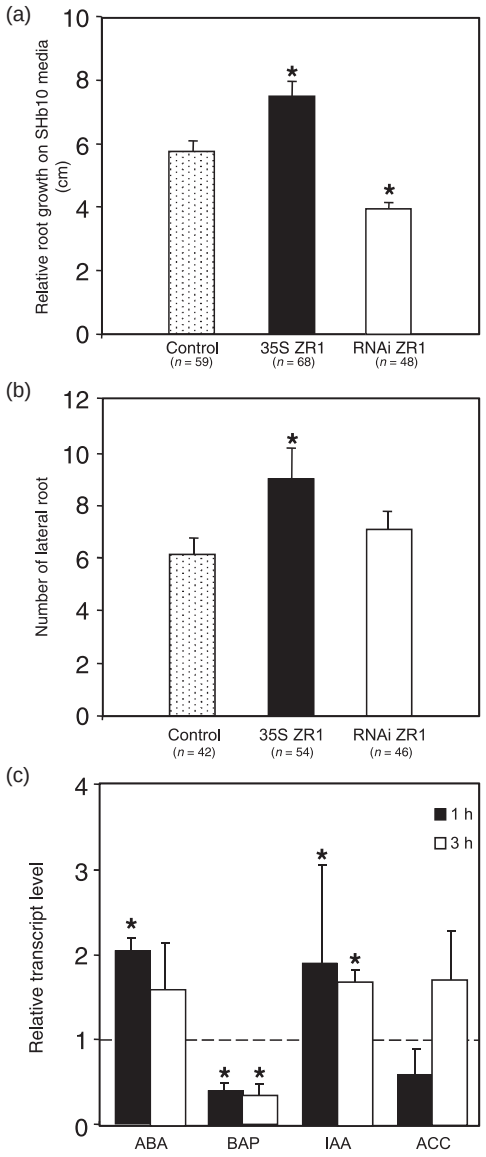

Figure 5. Changes in root development in transgenic roots after the modification of *MtZR1 MtZR1* expression by phytohormones. (a and b) Root growth and number of lateral roots from *P35S*::*GUS* (control, dotted box), *P35S*:*ZR1* (black box) and RNAi *MtZR1* (white box) after 2 weeks on SH10b agar medium. At least 48 root sections (each 1 cm long) from at least four independent transgenic root lines were aligned on an agar plate, and final root growth was measured after 2 weeks. Statistical analysis on the mean root growth and number of lateral roots was carried out by ANOVA, with $P < 0.05$ considered significant. The corresponding number of root samples is indicated in brackets (≥4 independent transgenic root lines for each construct). (c) *MtZR1* expression in roots after 3 h of hormone treatment: auxin (10^{-7} M IAA), cytokinin (10^{-7} M BAP), ethylene (10^{-7} M ACC) or abscisic acid (10^{-7} M ABA). Bars show the quantification of specific PCR amplification products for each gene, normalized against two constitutive genes (as described in Experimental procedures). Fold changes relative to the non-treated conditions are indicated by the dashed line. The mean of two biological replicates is shown, and error bars represent the standard deviation. Asterisks indicate values significantly different from those for non-treated conditions (*$P < 0.05$) based on REST 2009.

and *VPE* transcripts were similar in *ZR1*-overexpressing and control plants (Fig. 7b). By contrast, transcripts for these genes were significantly less abundant in nodules in which *ZR1* was silenced by RNAi than in control nodules (Fig. 7c). Thus, ZR1 can be considered to play an important role in the development of roots and nodules in *M. truncatula*.

DISCUSSION

ZR1 and *PRAF* genes in the *M. truncatula* genome

The goal of our study was to determine the importance of the ZR1 protein for the symbiotic interaction between *M. truncatula* and *S. meliloti*. We previously showed that *GmG93* is expressed only in infected cells of functional nodules, as the expression of this gene was not detected in other organs or in non-functional nodules (Clement *et al.* 2006). *GmG93* was shown to encode a protein of the PRAF family. This family contains proteins with multiple domains, suggesting roles in multiple functions in plants (Heras & Drobak 2002). The affinity of one of these domains, the FYVE domain of *A. thaliana*, for various phospholipids, including phosphatidylinositol-3-phosphate (PtdIns(3)P), has been studied *in vitro* (Jensen *et al.* 2001). We investigated the biological role of PRAF proteins in nodulation, by searching for sequences encoding PRAF proteins in the *M. truncatula* genome. We identified at least five members of the PRAF family, on the basis of predicted amino acid sequences, in *M. truncatula*. The gene most similar to *GmG93*, the nodule-specific PRAF gene, was *MtZR1*, which encoded a protein with an amino acid sequence 67% identical to that of the protein encoded by *GmG93*. *MtZR1* is also similar to *MsZR1*, which has been cloned from *M. sativa* and encodes a protein with a sequence 96% identical to that of *MtZR1*, suggesting that these genes are orthologous. We investigated the importance of *ZR1* in the leguminous model plant *M. truncatula*. *In silico* analysis of the expression profile of this gene carried out with Affymetrix *Medicago* Genome Array data (Benedito *et al.* 2008) showed that *ZR1* was weakly expressed in various plant organs (Supporting Information Fig. S2). RT-qPCR analysis confirmed the low-level expression of *ZR1* in roots, leaves and nodules. These findings strongly suggest that *ZR1* and *GmG93* are not orthologues, as *GmG93 expression* was detected only in nodules. However, steady-state *ZR1* transcript levels were significantly down-regulated in nodules subjected to abiotic stresses affecting nitrogen fixation efficiency, suggesting that the level of nodule *MtZR1* expression is associated with the nitrogen-fixing function of the nodule. An analysis of *MtZR1* promoter activity with the *PMtZR1::GUS* fusion in transgenic *M. truncatula* plants showed that *ZR1* was expressed in vascular bundles and, to a lesser extent, in the meristematic, infection and nitrogen-fixing zones of mature nodules. *ZR1* was also expressed in the infected zones of 2-week-old root nodules. The differing spatiotemporal patterns of *ZR1* expression suggest that this gene has different functions during nodule formation and functioning. Moreover, the

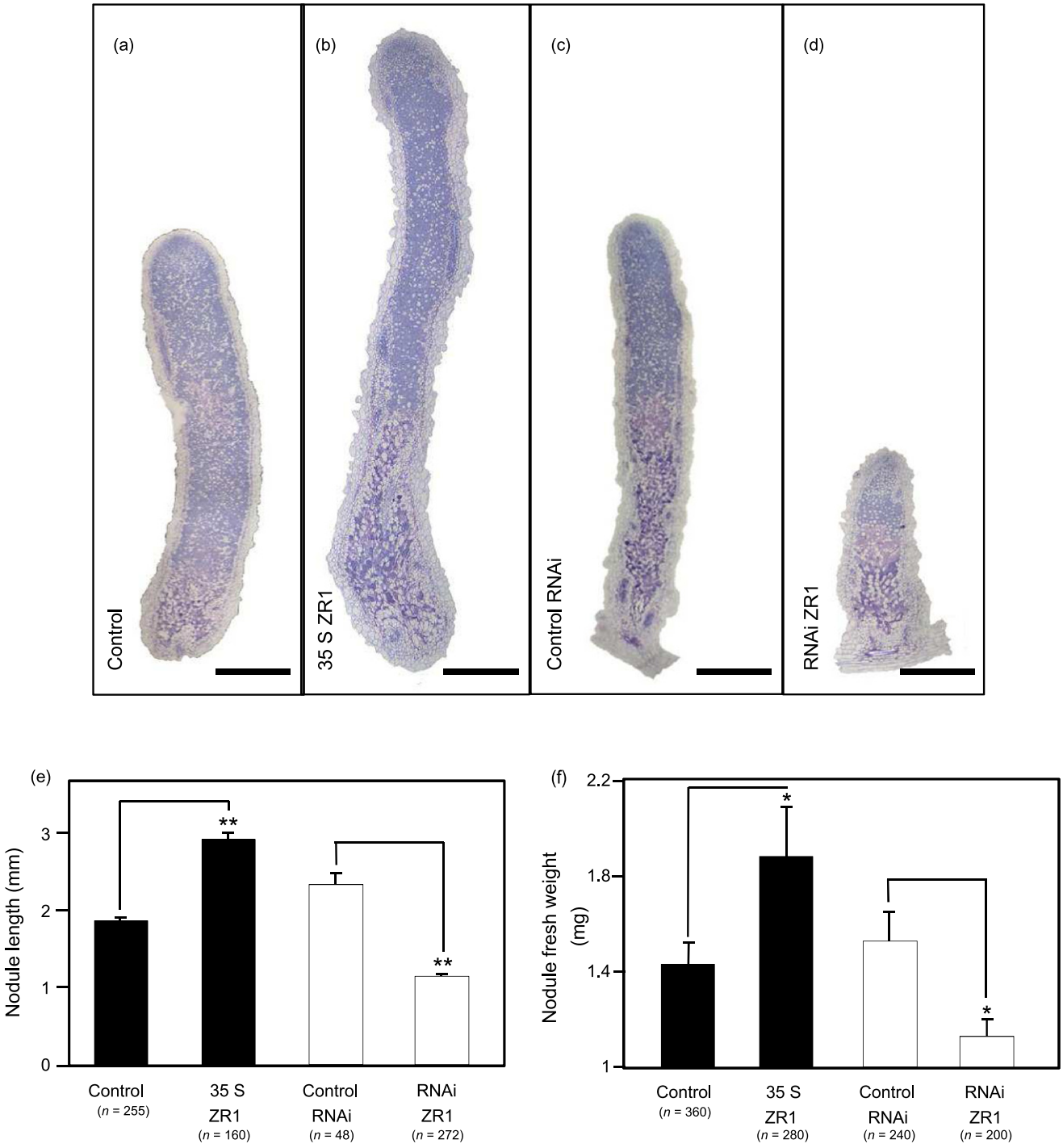

Figure 6. Comparison of the structural organization of symbiotic nodules after the deregulation of *MtZR1* expression. (a to d). Longitudinal section of transgenic root nodules from *M.truncatula* 6 weeks PI. Toluidine-*o*-blue-stained 5 μm sections from *P35S*::*GUS* (control, a) and *P35S*::*ZR1* (35S ZR1, b), empty RNAi vector (control RNAi, c) and RNAi *MtZR1* (RNAi ZR1, d) roots. Scale bars: 400 μm. (e) Nodule length and (f) nodule wet weight in composite plants in which *MtZR1* was overexpressed or silenced (control plants are *P35S*::*GUS* and RNAi *MtZR1*, respectively). In both cases, the mean of three biological replicates is shown ($n > 48$). Error bars represent the standard error of the mean and asterisks indicate significant differences relative to controls in a Mann–Whitney test ($*P < 0.05$; $**P < 0.01$).

expression of *ZR1* in the root meristem and during nodule development suggests a potential role in the development of these organs. As stated above, ZR1 is a multidomain protein with phospholipid-interacting (PH and FYVE), guanine exchange activity (ATS1/RCC1) and protein–protein interaction (BRX/DZC) domains (Jensen *et al.* 2001; Heras & Drobak 2002; Wywial & Singh 2010). Interactions between these different protein domains might mediate multiple

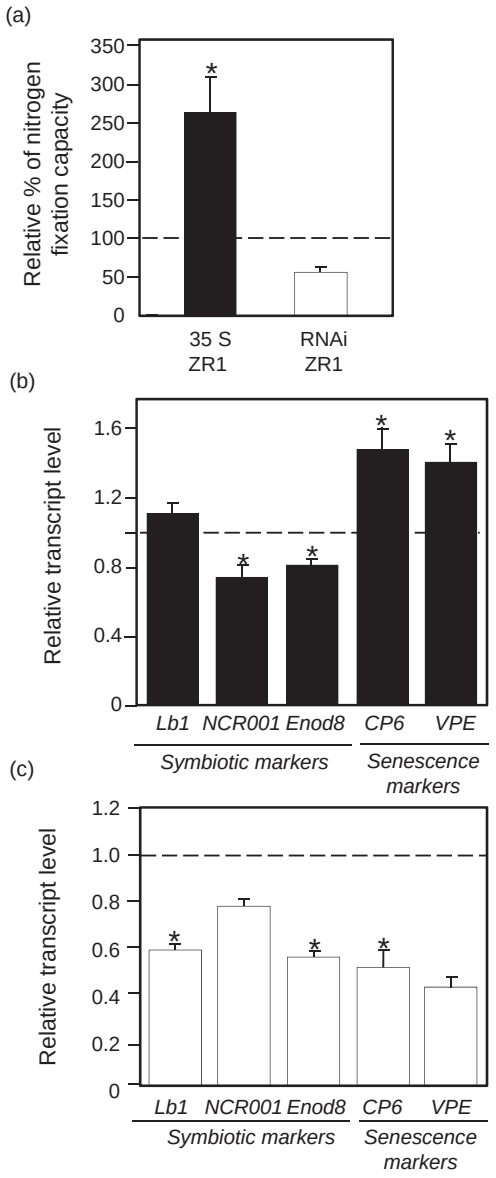

Figure 7. Biological nitrogen fixation and relative expression of symbiotic or senescence markers in transgenic nodules. (a) Nitrogen fixation (ARA) by root nodules in *P35S*::*ZR1* (black boxes) and RNAi *MtZR1* (white boxes), (normalized relative to *P35S*::*GUS* or empty RNAi vector control constructs, respectively, as indicated by the dashed line). Each bar indicates the standard error of the mean for five independent assays from three biological replicates. Statistical differences were assessed with the Kruskal–Wallis test, taking $P < 0.05$ to be significant (*). (b–c) Relative RT-qPCR analysis of symbiotic (*MtLb1*, *MtNCR001* and *MtEnod8*) and senescence (*MtCP6* and *MtVPE*) marker genes in transgenic root nodules overexpressing *MsZR1* (black boxes) or silenced for *MtZR1* (white boxes). The expression of each marker in control nodules was used to define fold changes (indicated by the dashed line). Error bars show the standard error of three experimental replicates from three biological experiments. PCR amplification was normalized against the mean value for two constitutive genes, *Mtc27* and *RP40S*. The stability of expression of the *Mtc27* and *RP40S* reference genes was checked with GeNorm software. The significance of differences was assessed with REST 2009, taking $P < 0.05$ to be significant (*).

cellular roles for ZR1 in root or nodule development and functioning.

ZR1 is involved in root and nodule development

We assessed the importance of ZR1 for root and nodule development, by implementing a genetic approach in *M. truncatula*. The overexpression of *ZR1* and the knockdown of the expression of this gene by RNAi of *ZR1* had significant, opposite effects on the development of both roots and symbiotic nodules. *ZR1* overexpression promoted root growth and the formation of lateral roots, whereas the RNAi-mediated knockdown of *ZR1* expression significantly decreased root growth. These results indicate that *ZR1* is required for normal root and nodule development. An analysis of *ZR1* expression under hormonal treatment showed a potential role of cytokinins, auxins and ABA in ZR1 regulation, as the expression of this gene was modified by treatment with these hormones. Crosstalk has been demonstrated between the auxin and cytokinin pathways, in the control of root development. Auxin is involved in the establishment and maintenance of the root apical meristem, whereas cytokinins decrease root apical meristem size and affect the rate of meristematic cell differentiation (reviewed by (Garay-Arroyo *et al.* 2012). Thus, the repression of *ZR1* expression in roots by cytokinins may affect meristem development. The detection of *ZR1* expression in the root tip and the meristems of lateral roots, and the larger number of lateral roots in *ZR1*-overexpressing root systems provide support for the notion that *ZR1* plays a role in meristematic cells. However, the number of nodules was not significantly affected in the transgenic roots, suggesting that ZR1 plays no significant role in nodule meristem formation. The opposite pattern of regulation by ABA provides support for the notion that *ZR1* and *GmG93* are not orthologues, as *GmG93* is down-regulated by ABA treatment (Clement *et al.* 2006). Nodule development and functioning were also modified by changes to *ZR1* expression. *ZR1* overexpression resulted in a larger nodule size and greater N_2 fixation capacity, whereas RNAi knockdown of *ZR1* expression resulted in significantly smaller nodules and lower nitrogen fixation efficiency. The significant differences observed in the expression of nodule gene markers for the nitrogen-fixing zone (*Lb1*, *NCR001* and *Enod 8*) and for senescence onset (*CP6* and *VPE*) revealed differences in nodule functioning with respect to control nodules. The higher levels of *CP6* and *VPE* expression, together with the lower levels of *NCR001* and *Enod 8* expression, in *ZR1*-overexpressing nodules may reflect a more advanced stage of nodule development, as suggested by the greater length of the nodule. The lower levels of expression of all the gene markers in RNAi-ZR1 nodules were also indicative of changes in the functioning of the nodule. Thus, *ZR1* plays a significant role, at least during nodule development. The observed changes in root and nodule development may reflect the regulatory role of the PH, FYVE, RCC1 and BRX protein domains. Indeed, a PH domain-containing protein (VAN3 ARF-GAP) has been shown to play a key role in plant vascular development, through the regulation of plant

venation continuity in *A. thaliana* (Naramoto *et al*. 2009). The PH domain is found in diverse proteins involved in cellular signalling, cytoskeleton organization, membrane trafficking and/or phospholipid modification (Lemmon 2004; Lindmo & Stenmark 2006). Both the PH and FYVE domains interact with phospholipids identified as regulatory lipids controlling various physiological processes in plants, such as root growth, pollen and vascular development (Ischebeck, Stenzel & Heilmann 2008; Lee *et al*. 2008). Finally, the cellular function of the multidomain ZR1 protein in *M. truncatula* could be investigated more completely by characterizing the other domains involved in protein–protein interactions: ATS1/RCC1 and BRX/DZC (Jensen *et al*. 2001; Mouchel, Briggs & Hardtke 2004; Wywial & Singh 2010). In *A. thaliana*, the activity of *AtPRAF1*RCC1 domains as guanine exchange factors has been investigated in interactions with small GTPase proteins (Arf, Rab and Ran) *in vitro*. Guanine exchange was found to be significantly catalysed on specific Rab proteins (Jensen *et al*. 2001). Such RCC1 domains can bind to the nucleosome in various organisms, from humans to plants, but we are only just beginning to understand the precise function of these domains (Hadjebi *et al*. 2008; Meier *et al*. 2008; Tan 2012). Finally, in *A. thaliana*, the BRX protein carrying a tandem repeat of the DZC domain has been shown to be produced in small amounts and to modulate root growth strongly (Mouchel *et al*. 2004). It would be interesting to investigate the potential interaction between BRX and ZR1 in *M. truncatula*, as an interaction between BRX and *At*PRAF1 has been demonstrated in *A. thaliana* (Briggs *et al*. 2006), and to investigate the effect of changes in BRX gene expression in transgenic roots and nodules.

In conclusion, this work provides the first evidence that ZR1, a member of the PRAF family, is required for normal root and nodule development in *M. truncatula*. Future studies will investigate the involvement of other *Mt*PRAF proteins in plant development and the symbiotic process.

ACKNOWLEDGMENTS

O. Pierre and T. Kazmierczak were the recipients of a doctoral grant from the 'Ministère de l'Education Nationale, de l'Enseignement Supérieur et de la Recherche'. We would like to thank Dr. K. Zwerger for providing the full-length cDNA of *MsZR1* (AJ409163) from *M. sativa*. We would like to thank C. Mura for providing tobacco plants. We thank L. Paganelli for providing us with BUBR1:GFP and BUB3.1:GFP. This manuscript was proof-read and rewritten by Alex Edelman & Associates and by Gloria Berrocal (BIOLUX). UMR ISA is a part of Labex Signalife.

REFERENCES

Alpizar E., Dechamp E., Espeout S., Royer M., Lecouls A.C., Nicole M., Bertrand B., Lashermes P. & Etienne H. (2006) Efficient production of *Agrobacterium rhizogenes*-transformed roots and composite plants for studying gene expression in coffee roots. *Plant Cell Reports* **25,** 959–967.

Ariel F., Diet A., Verdenaud M., Gruber V., Frugier F., Chan R. & Crespi M. (2010) Environmental regulation of lateral root emergence in *Medicago truncatula* requires the HD-Zip I transcription factor HB1. *The Plant Cell* **22,** 2171–2183.

Benedito V.A., Torres-Jerez I., Murray J.D., *et al*. (2008) A gene expression atlas of the model legume *Medicago truncatula*. *The Plant Journal* **55,** 504–513.

Boisson-Dernier A., Chabaud M., Garcia F., Becard G., Rosenberg C. & Barker D.G. (2001) *Agrobacterium rhizogenes*-transformed roots of *Medicago truncatula* for the study of nitrogen-fixing and endomycorrhizal symbiotic associations. *Molecular Plant-Microbe Interaction* **14,** 695–700.

Briggs G.C., Mouchel C.F. & Hardtke C.S. (2006) Characterization of the plant-specific BREVIS RADIX gene family reveals limited genetic redundancy despite high sequence conservation. *Plant Physiology* **140,** 1306–1316.

Caillaud M.C., Paganelli L., Lecomte P., Deslandes L., Quentin M., Pecrix Y., Le Bris M., Marfaing N., Abad P. & Favery B. (2009) Spindle assembly checkpoint protein dynamics reveal conserved and unsuspected roles in plant cell division. *PLoS ONE* **4,** e6757.

Chomczynski P. & Sacchi N. (1987) Single-step method of RNA isolation by acid guanidinium thiocyanate-phenol-chloroform extraction. *Analytical Biochemistry* **162,** 156–159.

Clement M., Boncompagni E., de Almeida-Engler J. & Herouart D. (2006) Isolation of a novel nodulin: a molecular marker of osmotic stress in *Glycine max/Bradyrhizobium japonicum* nodule. *Plant, Cell & Environment* **29,** 1841–1852.

Coque L., Neogi P., Pislariu C., Wilson K.A., Catalano C., Avadhani M., Sherrier D.J. & Dickstein R. (2008) Transcription of ENOD8 in *Medicago truncatula* nodules directs ENOD8 esterase to developing and mature symbiosomes. *Molecular Plant-Microbe Interaction* **21,** 404–410.

Dereeper A., Guignon V., Blanc G., *et al*. (2008) Phylogeny.fr: robust phylogenetic analysis for the non-specialist. *Nucleic Acids Research* **36,** W465–W469.

El Msehli S., Lambert A., Baldacci-Cresp F., Hopkins J., Boncompagni E., Smiti S.A., Herouart D. & Frendo P. (2011) Crucial role of (homo)glutathione in nitrogen fixation in *Medicago truncatula* nodules. *New Phytologist* **192,** 496–506.

Favery B., Complainville A., Vinardell J.M., Lecomte P., Vaubert D., Mergaert P., Kondorosi A., Kondorosi E., Crespi M. & Abad P. (2002) The endosymbiosis-induced genes ENOD40 and CCS52a are involved in endoparasitic-nematode interactions in *Medicago truncatula*. *Molecular Plant-Microbe Interaction* **15,** 1008–1013.

Fedorova M., van de Mortel J., Matsumoto P.A., Cho J., Town C.D., VandenBosch K.A., Gantt J.S. & Vance C.P. (2002) Genome-wide identification of nodule-specific transcripts in the model legume *Medicago truncatula*. *Plant Physiology* **130,** 519–537.

Garay-Arroyo A., De La Paz Sanchez M., Garcia-Ponce B., Azpeitia E. & Alvarez-Buylla E.R. (2012) Hormone symphony during root growth and development. *Developmental Dynamics* **241,** 1867–1885.

Gibson K.E., Kobayashi H. & Walker G.C. (2008) Molecular determinants of a symbiotic chronic infection. *Annual Review of Genetics* **42,** 413–441.

Gonzalez-Rizzo S., Crespi M. & Frugier F. (2006) The *Medicago truncatula* CRE1 cytokinin receptor regulates lateral root development and early symbiotic interaction with *Sinorhizobium meliloti*. *The Plant Cell* **18,** 2680–2693.

Hadjebi O., Casas-Terradellas E., Garcia-Gonzalo F.R. & Rosa J.L. (2008) The RCC1 superfamily: from genes, to function, to disease. *Biochimica et Biophysica ACTA* **1783,** 1467–1479.

Hatsugai N., Kuroyanagi M., Yamada K., Meshi T., Tsuda S., Kondo M., Nishimura M. & Hara-Nishimura I. (2004) A plant vacuolar protease, VPE, mediates virus-induced hypersensitive cell death. *Science* **305,** 855–858.

Heras B. & Drobak B.K. (2002) PARF-1: an *Arabidopsis thaliana* FYVE-domain protein displaying a novel eukaryotic domain structure and phosphoinositide affinity. *Journal of Experimental Botany* **53,** 565–567.

Ischebeck T., Stenzel I. & Heilmann I. (2008) Type B phosphatidylinositol-4-phosphate 5-kinases mediate *Arabidopsis* and *Nicotiana tabacum* pollen tube growth by regulating apical pectin secretion. *The Plant Cell* **20,** 3312–3330.

Jensen R.B., La Cour T., Albrethsen J., Nielsen M. & Skriver K. (2001) FYVE zinc-finger proteins in the plant model *Arabidopsis thaliana*: identification of PtdIns3P-binding residues by comparison of classic and variant FYVE domains. *Biochemical Journal* **359,** 165–173.

Jones K.M., Kobayashi H., Davies B.W., Taga M.E. & Walker G.C. (2007) How rhizobial symbionts invade plants: the *Sinorhizobium-Medicago* model. *Nature Reviews Microbiology* **5,** 619–633.

Journet E.P., Pichon M., Dedieu A., de Billy F., Truchet G. & Barker D.G. (1994) *Rhizobium meliloti* Nod factors elicit cell-specific transcription of the ENOD12 gene in transgenic alfalfa. *The Plant Journal* **6,** 241–249.

Journet E.P., van Tuinen D., Gouzy J., *et al*. (2002) Exploring root symbiotic programs in the model legume *Medicago truncatula* using EST analysis. *Nucleic Acids Research* **30,** 5579–5592.

Lazo G.R., Stein P.A. & Ludwig R.A. (1991) A DNA transformation-competent *Arabidopsis* genomic library in Agrobacterium. *Biotechnology (N Y)* **9,** 963–967.

Lee Y., Bak G., Choi Y., Chuang W.I., Cho H.T. & Lee Y. (2008) Roles of Phosphatidylinositol 3-kinase in root hair growth. *Plant Physiology* **147,** 624–635.

van Leeuwen W., Okresz L., Bogre L. & Munnik T. (2004) Learning the lipid language of plant signalling. *Trends in Plant Science* **9,** 378–384.

Lemmon M.A. (2004) Pleckstrin homology domains: not just for phosphoinositides. *Biochemical Society Transactions* **32,** 707–711.

Lindmo K. & Stenmark H. (2006) Regulation of membrane traffic by phosphoinositide 3-kinases. *Journal of Cell Science* **119,** 605–614.

Livak K.J. & Schmittgen T.D. (2001) Analysis of relative gene expression data using real-time quantitative PCR and the 2(-Delta Delta C(T)) method. *Methods* **25,** 402–408.

Matamoros M.A., Baird L.M., Escuredo P.R., Dalton D.A., Minchin F.R., Iturbe-Ormaetxe I., Rubio M.C., Moran J.F., Gordon A.J. & Becana M. (1999) Stress-induced legume root nodule senescence. Physiological, biochemical, and structural alterations. *Plant Physiology* **121,** 97–112.

Meier I., Xu X.M., Brkljacic J., Zhao Q. & Wang H.J. (2008) Going green: plants' alternative way to position the Ran gradient. *Journal of Microscopy* **231,** 225–233.

Mergaert P., Nikovics K., Kelemen Z., Maunoury N., Vaubert D., Kondorosi A. & Kondorosi E. (2003) A novel family in *Medicago truncatula* consisting of more than 300 nodule-specific genes coding for small, secreted polypeptides with conserved cysteine motifs. *Plant Physiology* **132,** 161–173.

Mouchel C.F., Briggs G.C. & Hardtke C.S. (2004) Natural genetic variation in *Arabidopsis* identifies BREVIS RADIX, a novel regulator of cell proliferation and elongation in the root. *Genes and Development* **18,** 700–714.

Naramoto S., Sawa S., Koizumi K., Uemura T., Ueda T., Friml J., Nakano A. & Fukuda H. (2009) Phosphoinositide-dependent regulation of VAN3 ARF-GAP localization and activity essential for vascular tissue continuity in plants. *Development* **136,** 1529–1538.

Oldroyd G.E., Murray J.D., Poole P.S. & Downie J.A. (2011) The rules of engagement in the legume-rhizobial symbiosis. *Annual Review of Genetics* **45,** 119–144.

Osteras M., Boncompagni E., Vincent N., Poggi M.C. & Le Rudulier D. (1998) Presence of a gene encoding choline sulfatase in *Sinorhizobium meliloti bet* operon: choline-O-sulfate is metabolized into glycine betaine. *Proceedings of the National Academy of Sciences of the United States of America* **95,** 11394–11399.

Ott T., van Dongen J.T., Gunther C., Krusell L., Desbrosses G., Vigeolas H., Bock V., Czechowski T., Geigenberger P. & Udvardi M.K. (2005) Symbiotic leghemoglobins are crucial for nitrogen fixation in legume root nodules but not for general plant growth and development. *Current Biology* **15,** 531–535.

Pfaffl M.W., Horgan G.W. & Dempfle L. (2002) Relative expression software tool (REST) for group-wise comparison and statistical analysis of relative expression results in real-time PCR. *Nucleic Acids Research* **30,** e36.

Plet J., Wasson A., Ariel F., Le Signor C., Baker D., Mathesius U., Crespi M. & Frugier F. (2011) MtCRE1-dependent cytokinin signaling integrates bacterial and plant cues to coordinate symbiotic nodule organogenesis in *Medicago truncatula*. *The Plant Journal* **65,** 622–633.

Puppo A., Dimitrijevic L. & Rigaud J. (1982) Possible involvement of nodule superoxide dismutase and catalase in leghemoglobin protection. *Planta* **156,** 374–379.

Ramos J. & Bisseling T. (2003) A method for the isolation of root hairs from the model legume *Medicago truncatula*. *Journal of Experimental Botany* **54,** 2245–2250.

Staudinger C., Mehmeti V., Turetschek R., Lyon D., Egelhofer V. & Wienkoop S. (2012) Possible role of nutritional priming for early salt and drought stress responses in *Medicago truncatula*. *Frontiers in Plant Science* **3,** 285.

Takase T., Yanagawa Y., Komatsu S., Nakagawa H. & Hashimoto J. (2003) Cell-cycle-related variation in proteins in suspension-cultured rice cells. *Plant Disease Research* **116,** 469–475.

Tan S. (2012) Deciphering how the chromatin factor RCC1 recognizes the nucleosome: the importance of individuals in the scientific discovery process. *Biochemical Society Transactions* **40,** 351–356.

Timmers A.C., Soupene E., Auriac M.C., de Billy F., Vasse J., Boistard P. & Truchet G. (2000) Saprophytic intracellular rhizobia in alfalfa nodules. *Molecular Plant-Microbe Interactions* **13,** 1204–1213.

Van de Velde W., Guerra J.C., De Keyser A., De Rycke R., Rombauts S., Maunoury N., Mergaert P., Kondorosi E., Holsters M. & Goormachtig S. (2006) Aging in legume symbiosis. A molecular view on nodule senescence in *Medicago truncatula*. *Plant Physiology* **141,** 711–720.

Vandesompele J., De Preter K., Pattyn F., Poppe B., Van Roy N., De Paepe A. & Speleman F. (2002) Accurate normalization of real-time quantitative RT-PCR data by geometric averaging of multiple internal control genes. *Genome Biology* **3,** research0034.1–research0034.11.

Vieweg M.F., Fruhling M., Quandt H.J., Heim U., Baumlein H., Puhler A., Kuster H. & Andreas M.P. (2004) The promoter of the *Vicia faba* L. leghemoglobin gene *VfLb29* is specifically activated in the infected cells of root nodules and in the arbuscule-containing cells of mycorrhizal roots from different legume and nonlegume plants. *Molecular Plant-Microbe Interactions* **17,** 62–69.

Voinnet O., Rivas S., Mestre P. & Baulcombe D. (2003) An enhanced transient expression system in plants based on suppression of gene silencing by the p19 protein of tomato bushy stunt virus. *The Plant Journal* **33,** 949–956.

Wywial E. & Singh S.M. (2010) Identification and structural characterization of FYVE domain-containing proteins of *Arabidopsis thaliana*. *BMC Plant Biology* **10,** 157.

Received 30 May 2013; received in revised form 1 August 2013; accepted for publication 5 August 2013

SUPPORTING INFORMATION

Additional Supporting Information may be found in the online version of this article at the publisher's web-site:

Figure S1. ClustalW alignment of the *Mt*ZR1 and *Ms*ZR1 protein sequences. The consensus sequences are marked with a star.

Figure S2. Gene atlas profile of Affymetrix Probeset ID of *M. truncatula* PRAF genes (Mtr.35761.1.S1_at, in red (MtPRAFChr1); Mtr.20584.1.S1_at, in blue (MtPRAFChr5), Msa.965.1.S1_at, in pink (MtZR1); Mtr.14364.1.S1_at, in purple (MtPRAFChr0) and Mtr.47635.1.S1_at, in black (MtPRAFChr1).

Figure S3. GUS staining of *P35S*::*GUS* and *PMtZR1*::*GFP*::*GUS* transgenic root nodules.

(a to b). Insets show the overall GUS staining of the uncut root nodule. A. *P35S*::*GUS*, GUS staining of a 70 μm-thick section of a six-week-old nodule showing *GUS* expression in all root tissues and in the nodule vascular bundles (black arrow). Staining within the nodule is essentially restricted to uninfected cells (III). Zones I to IV: Functional zones in the mature nodule. B. *PMtZR1*::*GFP*::*GUS*, six-week-old nodule showing the overall expression pattern for *GUS* under the control of the *MtZR1* promoter. GUS staining is restricted to the nodule vascular bundle (black arrows) and the junction between the root and the nodule. Scale bars: 400 μm (a and b).

Figure S4. Analysis of *MtZR1* expression in transgenic roots or nodules in which *MtZR1* was overexpressed or silenced. (a) Analysis of *MtZR1* expression in roots overexpressing *ZR1* (35S ZR1) or *MtZR1* RNAi (RNAi ZR1). (b) Analysis of *MtZR1* expression in nodules overexpressing *ZR1* (35S ZR1) or *MtZR1* RNAi (RNAi ZR1). The respective controls, P35S::GUS and RNAi empty vector, were used as calibrators to define fold-changes (indicated by the broken line). RT-qPCR values were normalised against the mean value for two constitutively expressed genes (*Mtc27* and *RP40S*). Error bars show the standard error of 3 experimental replicates from 3 biological experiments. The significance of

differences was assessed with REST 2009, taking $P < 0.05$ to be significant (*).

Figure S5. Relative RT-qPCR analysis of *MtPRAF* expression in transgenic root nodules overexpressing *MsZR1* (a) or subject to RNAi-mediated *MtZR1* silencing (b). Values are representative of three independent biological replicates. Gene expression values were normalised against *Mtc27*. No PCR amplification was detectable for *MtPRAF* genes AC1413228_41.4 and AC151619_14.4.

Figure S6. Nodule number in composite plants in which *MtZR1* was overexpressed or silenced. Relative numbers of nodules on roots overexpressing *ZR1* (35S ZR1, black box) or *MtZR1* RNAi (RNAi ZR1, white box). The number of nodules in control plants is indicated by the dashed line. Error bars show the standard error of at least 12 experimental replicates from 2 biological experiments.

Table S1. *Medicago* PRAF Gene ID and Affymetrix Probeset ID.

Table S2. Bacterial strains and plasmids.

Table S3. Primer list for Gateway constructs and RT-qPCR.